

Measuring Densities of Solids and Liquids Using Magnetic Levitation: Fundamentals

Katherine A. Mirica, Sergey S. Shevkoplyas, Scott T. Phillips, Malancha Gupta, and George M. Whitesides*

Department of Chemistry and Chemical Biology, Harvard University, 12 Oxford Street, Cambridge, Massachusetts 02138

Received February 5, 2009; E-mail: gwhitesides@gmwgroup.harvard.edu

Abstract: This paper describes an analytical system that uses magnetic levitation to measure densities of solids and water-immiscible organic liquids with accuracies ranging from ± 0.0002 to ± 0.02 g/cm³, depending on the type of experiment. The technique is compatible with densities of 0.8–3 g/cm³ and is applicable to samples with volumes of 1 pL to 1 mL; the samples can be either spherical or irregular in shape. The method employs two permanent NdFeB magnets positioned with like poles facing one another—with the axis between the poles aligned with the gravitational field—and a container filled with paramagnetic medium (e.g., MnCl₂ dissolved in water) placed between these magnets. Density measurements are obtained by placing the sample into the container and measuring the position of the sample relative to the bottom magnet. The balance of magnetic and gravitational forces determines the vertical position of the sample within the device; knowing this position makes it possible to calculate the density of the sample.

Introduction

This article describes the use of magnetic levitation to measure densities of solids and liquids accurately (accuracy ranging from ± 0.0002 to ± 0.02 g/cm³, depending on the choice of experimental conditions) and quickly (~ 10 s for objects with diameters > 500 μm). The method requires only a capillary tube (or a vial) that contains a paramagnetic solution (Mn²⁺ or Gd³⁺ in water) and two permanent NdFeB magnets oriented with like poles facing one another (Figure 1). We measure the density of a diamagnetic solid particle and a droplet of organic liquid by suspending it in this aqueous paramagnetic solution and then placing the vial containing the solution between the two magnets (with the axis perpendicular to the face of the magnets and coaxial with the gravitational field). The balance of gravitational and magnetic forces determines the equilibrium position of every particle between the magnets; we use these positions to calculate the densities of the particles (Figure 1).

The method is compatible with most types of solids and water-insoluble organic liquids with densities in the range 0.8–3 g/cm³, does not require a measurement of volume or mass of the analyte, is applicable to samples with volumes ranging from 1 pL to 1 mL, and can be used to measure densities of several different samples simultaneously.

We implement this method of measuring density by (i) using calibration plots based on comparison of unknowns with particles (e.g., glass density standards, polymers) or droplets of known densities and (ii) using an analytical expression derived from the theory of magnetic levitation. The convenient feature of comparing unknowns with calibration curves is that this approach does not require the exact knowledge of various experimental parameters and allows the user to neglect most of the physics of magnetic levitation. We demonstrate the accuracy of each approach by measuring densities of glass beads with precisely known densities

(± 0.0002 g/cm³), spherically and irregularly shaped particles of several polymers, and water-insoluble organic droplets. This article also describes the fundamental limitations of this technique. We infer that (i) the technique (using the device we describe here) cannot measure densities of objects smaller than ~ 2 μm in radius, (ii) the time required for a measurement depends upon the size of the sample object, (iii) measurements of density are temperature-dependent, (iv) the most accurate measurements (± 0.0002 g/cm³) are obtained when the approximate density of the sample is already known, because high-sensitivity protocols are applicable only over narrow ranges of densities, and (v) the method is not compatible with samples that dissolve in aqueous paramagnetic medium.

Every substance has density, and many physical and chemical processes are accompanied by changes in density. We believe that a method of measuring density that is inexpensive, accurate, rapid, convenient, and applicable to small (< 1 cm³) volumes of sample will be broadly useful. Current techniques for measuring densities—hydrostatic weighing, pycnometry, density-gradient columns, and oscillating tube technology¹—are often inconvenient, are not applicable to certain types of samples, involve substantial technical skill, and require access to expensive equipment.

This paper describes measurement of densities using magnetic levitation. The device we use is portable and inexpensive (the NdFeB magnets cost \sim \$5 each),² operates without electricity, and requires no additional external equipment (we perform measurements using a standard ruler with millimeter scale markings). The prototype device

- (1) Webster, J. G., Ed. *The Measurement, Instrumentation, and Sensors Handbook*; CRC Press and IEEE Press: Boca Raton, FL, 1999.
- (2) This is bulk pricing; individual 5 cm \times 5 cm \times 2.5 cm NdFeB magnets are available for \$15–20 at www.magnet4less.com.

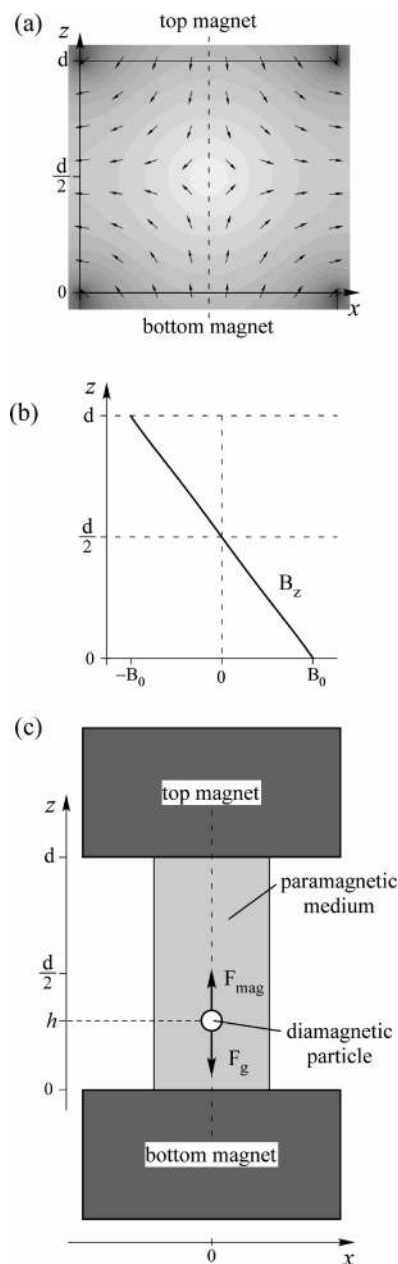


Figure 1. Theory of magnetic levitation. (a) A 2D numerical simulation (COMSOL Multiphysics) of the magnetic field, B , between two identical permanent magnets ($5 \text{ cm} \times 5 \text{ cm} \times 2.5 \text{ cm}$) separated by $d = 4.5 \text{ cm}$ and arranged in an anti-Helmholtz configuration (i.e., with like poles facing each other). Arrows point in the direction of the field ($(B)/|B|$), and the grayscale contour plot indicates the magnitude of the field ($|B|$); darker shades correspond to stronger field. (b) The magnitude of the z component of the magnetic field vector, B_z , along the centerline (dotted line in panel a); B_0 is the magnitude of the magnetic field in the center of the top surface of the bottom magnet in the configuration shown in panel a. For NdFeB magnets that are $5 \text{ cm} \times 5 \text{ cm} \times 2.5 \text{ cm}$ in size, the dependence of B_z on z is approximately linear ($R^2 = 0.9999$) when the separation between the magnets is about 45 mm or less. (c) Schematic illustration of the experimental setup; the y -axis points into the plane of the image and is not shown.

measures $8 \text{ cm} \times 6 \text{ cm} \times 12 \text{ cm}$, although the use of smaller magnets and smaller supports for the magnets would enable further miniaturization. These characteristics make magnetic levitation well-suited for performing density measurements in resource-limited environments.

We and others have used magnetic levitation in the past for trapping small objects and separating diamagnetic materials on

the basis of differences in density.^{3–18} Magnetic levitation has not, to the best of our knowledge, been developed into a convenient method for measuring densities in analytical contexts.

Magnetic levitation was developed in the 1960s for density-based separations of minerals, metals, and plastics suspended in ferrofluids or solutions of paramagnetic salts.³ Separation of diamagnetic substances also has been achieved in pressurized oxygen with superconducting magnets ($\sim 10 \text{ T}$); examples include separation of NaCl from KCl,¹⁰ colored glass particles of different densities,¹⁰ and biological materials, such as hemoglobin, cholesterol, and DNA,⁸ as well as collagens obtained from different sources.¹⁸ Catherall and co-workers separated pieces of silicon, gallium arsenide, lead, and gold by levitating these objects in liquid oxygen at atmospheric pressure using magnetic fields in the range of $0.7\text{--}17 \text{ T}$.¹⁹

The use of magnetic levitation in compact systems for density-based separations using readily available ($\sim 1 \text{ T}$) magnetic fields has been reported recently. Kimura and colleagues demonstrated separation of a number of polymers using aqueous solutions of MnCl_2 and an electromagnet that generated a magnetic field of 2.1 T .¹² We described a device consisting of two permanent magnets ($\sim 0.4 \text{ T}$) and aqueous solutions of Gd^{3+} ions that we used for density-based separation of polymers and for detection of binding interactions, including the electrostatic adsorption of gold nanoparticles to polymeric microspheres and the binding of streptavidin to solid-supported biotin.¹⁷ We also used this device to distinguish atomic-level differences in chemical composition of polymers and to monitor the progress and kinetics of chemical reactions on solid supports.¹⁵

Experimental Design

Theory of Magnetic Levitation. Magnetic levitation measures densities by exploiting the balance between the magnetic force (which depends on the magnetic properties of the objects and of the suspending medium) and the gravitational force (which depends on the densities of the objects and of the medium). Most materials are diamagnetic and interact only weakly with a magnetic field.²⁰

- (3) Andres, U. *Magnetohydrodynamic & Magnetohydrostatic Methods of Mineral Separation*; John Wiley & Sons: New York, NY, 1976.
- (4) Beaugnon, E.; Tournier, R. *Nature* **1991**, *349*, 470–470.
- (5) Catherall, A. T.; Lopez-Alcaraz, P.; Benedict, K. A.; King, P. J.; Eaves, L. *New J. Phys.* **2005**, *7*, No. 118.
- (6) Feinstein, E.; Prentiss, M. *J. Appl. Phys.* **2006**, *99*, 064901.
- (7) Guevorkian, K.; Valles, J. M. *Proc. Natl. Acad. Sci. U.S.A.* **2006**, *103*, 13051–13056.
- (8) Hirota, N.; Kurashige, M.; Iwasaka, M.; Ikehata, M.; Uetake, H.; Takayama, T.; Nakamura, H.; Ikezoe, Y.; Ueno, S.; Kitazawa, K. *Physica B* **2004**, *346*, 267–271.
- (9) Ikezoe, Y.; Hirota, N.; Nakagawa, J.; Kitazawa, K. *Nature* **1998**, *393*, 749–750.
- (10) Ikezoe, Y.; Kaihatsu, T.; Sakae, S.; Uetake, H.; Hirota, N.; Kitazawa, K. *Energy Conv. Manag.* **2002**, *43*, 417–425.
- (11) Kimura, T. *Polym. J.* **2003**, *35*, 823–843.
- (12) Kimura, T.; Mamada, S.; Yamato, M. *Chem. Lett.* **2000**, 1294–1295.
- (13) Lyuksyutov, I. F.; Lyuksyutova, A.; Naugle, D. G.; Rathnayaka, K. D. D. *Mod. Phys. Lett. B* **2003**, *17*, 935–940.
- (14) Lyuksyutov, I. F.; Naugle, D. G.; Rathnayaka, K. D. D. *Appl. Phys. Lett.* **2004**, *85*, 1817–1819.
- (15) Mirica, K. A.; Phillips, S. T.; Shevkoplyas, S. S.; Whitesides, G. M. *J. Am. Chem. Soc.* **2008**, *130*, 17678–17680.
- (16) Valles, J. M.; Lin, K.; Denegre, J. M.; Mowry, K. L. *Biophys. J.* **1997**, *73*, 1130–1133.
- (17) Winkleman, A.; Perez-Castillejos, R.; Gudiksen, K. L.; Phillips, S. T.; Prentiss, M.; Whitesides, G. M. *Anal. Chem.* **2007**, *79*, 6542–6550.
- (18) Yokoyama, K.; Hirota, N.; Iwasaka, M. *IEEE Trans. Appl. Supercond.* **2007**, *17*, 2181–2184.
- (19) Catherall, A. T.; Eaves, L.; King, P. J.; Booth, S. R. *Nature* **2003**, *422*, 579–579.
- (20) Lide, D. R., Ed. *CRC Handbook of Chemistry and Physics*, 89th ed. [Online]; CRC Press: Boca Raton, FL, 2008.

A simple way to enable weakly diamagnetic objects to respond to an applied magnetic field is to suspend them in a solution of a strongly paramagnetic ion.³ Aqueous solutions of various paramagnetic substances, such as MnCl₂, MnBr₂, GdCl₃, CuSO₄, FeCl₂, and HoCl₃, can be used for levitating diamagnetic objects (Figure S1 in the Supporting Information).³ By using different paramagnetic salts, it is possible to vary the densities and magnetic susceptibilities of solutions of these salts independently. It is, therefore, possible to provide a high degree of control over both magnetic and gravitational forces.

In this study, we used aqueous solutions of MnCl₂ or GdCl₃ as the suspending media because they (i) have high molar magnetic susceptibilities ($\chi_{\text{MnCl}_2} = 14350 \times 10^{-6} \text{ cm}^3/\text{mol}$ and $\chi_{\text{GdCl}_3} = 27930 \times 10^{-6} \text{ cm}^3/\text{mol}$),²⁰ (ii) form transparent solutions in water that permit straightforward visualization of samples, and (iii) are relatively inexpensive (<\$0.01 per gram of MnCl₂, and \$0.34 per gram of GdCl₃).²¹

Equation 1 gives the magnetic force, \vec{F}_{mag} (N), acting on a diamagnetic object suspended in a paramagnetic solution under an applied magnetic field, \vec{B} (T).²² In this equation, χ_m (unitless) is the magnetic susceptibility of the paramagnetic medium and χ_s (unitless) is the magnetic susceptibility of the suspended object, $\mu_0 = 4\pi \times 10^{-7} \text{ (N}\cdot\text{A}^{-2})$ is the magnetic permeability of free space, and V (m³) is the volume of the object. Equation 2 provides the expression for the force of gravity, \vec{F}_g (N), acting on the suspended object; in this equation, ρ_s is the density of the object, ρ_m is the density of the medium, and \vec{g} is the vector of gravity. It follows from eq 3 that, in a stationary fluid, the object will come to rest if at any point the vector sum of the magnetic force \vec{F}_{mag} (eq 1) and the force of gravity \vec{F}_g (eq 2) becomes zero (eq 4). (In eq 3, \vec{a} is the acceleration of the object, m is the mass of the object, and \vec{F}_d is the force of the viscous drag experienced by the object.)

$$\vec{F}_{\text{mag}} = \frac{(\chi_s - \chi_m)}{\mu_0} V(\vec{B} \cdot \vec{\nabla})\vec{B} \quad (1)$$

$$\vec{F}_g = (\rho_s - \rho_m)V\vec{g} \quad (2)$$

$$m\vec{a} = \vec{F}_{\text{mag}} + \vec{F}_g + \vec{F}_d \quad (3)$$

$$\vec{F}_g + \vec{F}_{\text{mag}} = (\rho_s - \rho_m)V\vec{g} + \frac{(\chi_s - \chi_m)}{\mu_0} V(\vec{B} \cdot \vec{\nabla})\vec{B} = 0 \quad (4)$$

The force of gravity (corrected for the effect of buoyancy) is always directed to or away from the center of the Earth. The magnitude of the gravitational force, therefore, does not depend on the position of the object as long as the densities of the paramagnetic medium and the object remain constant. In a 3D Cartesian coordinate system in which the z -axis is aligned with the direction of the vector of gravity, $\vec{g} = (0, 0, -g)$ (as is shown in Figure 1c), the balance of forces (eq 4) simplifies to yield eq 5, because these two forces balance each other only along the z -axis.

$$-(\rho_s - \rho_m)g + \frac{(\chi_s - \chi_m)}{\mu_0} \left(B_x \frac{\partial B_z}{\partial x} + B_y \frac{\partial B_z}{\partial y} + B_z \frac{\partial B_z}{\partial z} \right) = 0 \quad (5)$$

Design of the Device. We established the magnetic field in our system by aligning two indistinguishable ~ 0.4 T NdFeB magnets

(5 cm \times 5 cm \times 2.5 cm) coaxially, 4.5 cm apart, with like poles facing one another—the so-called *anti-Helmholtz* configuration (Figure 1). We chose to use *permanent* magnets rather than *electromagnets* for simplicity: permanent magnets are inexpensive and portable, and require no electricity to operate.

The exact analytical expression describing the magnetic field between two identical rectangular permanent magnets in an anti-Helmholtz configuration in 3D is fairly complicated.^{23,24} Because of the symmetry, the x - and y -axes in our system are equivalent—that is, the distributions of magnetic field between the magnets in the zx and in the zy planes are identical. A simple numerical simulation of the magnetic field between the magnets performed in 2D (COMSOL Multiphysics, COMSOL, Inc., Burlington, MA) yields a well-known result for the distribution of the field in the zx plane (Figure 1a).²⁵

Our simulation shows that, along the centerline, the absolute value of the third term in eq 5 ($B_z(\partial B_z/\partial z)$) is at least 10^3 times larger than the absolute value of the sum of the first and second terms ($B_x(\partial B_z/\partial x) + B_y(\partial B_z/\partial y)$). With the magnets we used (NdFeB, 5 cm \times 5 cm \times 2.5 cm), B_z varies virtually linearly ($R^2 = 0.9999$) with z (the distance from the surface of the bottom magnet), from a maximum of $+B_0$ at the surface of the bottom magnet ($z = 0$) to a minimum of $-B_0$ at the surface of the top magnet ($z = d$) (Figure 1b), if the separation between the magnets, d , is less than or equal to approximately 45 mm (see Figure S0 in the Supporting Information). Because of this linearity, we can approximate the magnetic field along the centerline with eq 6.

$$\vec{B} \equiv \begin{pmatrix} B_x \\ B_y \\ B_z \end{pmatrix} = \begin{pmatrix} 0 \\ 0 \\ -\frac{2B_0}{d}z + B_0 \end{pmatrix} \quad (6)$$

Dependence of Sample Density on Levitation Height. We can solve eq 5 using the explicit expression for the magnetic field (eq 6) to find the equilibrium point, h (m), between the two magnets where the force of gravity and the magnetic force acting on the object balance each other (eq 7). It follows from eq 7 that there is a linear relationship between the density of the object, ρ_s , and its equilibrium position above the surface of the bottom magnet—the levitation height— h , which is given by eq 8a.

$$h = \frac{(\rho_s - \rho_m)g\mu_0 d^2}{(\chi_s - \chi_m)4B_0^2} + \frac{d}{2} \quad (7)$$

$$\rho_s = \alpha h + \beta \quad (8a)$$

$$\alpha = \frac{4(\chi_s - \chi_m)B_0^2}{g\mu_0 d^2} \quad (8b)$$

$$\beta = \rho_m - \frac{2(\chi_s - \chi_m)B_0^2}{g\mu_0 d} \quad (8c)$$

Equilibration Time. To find the time it takes a spherical particle of radius R (m) to move from one position z_i (e.g., at the bottom of the cuvette) to another position z_f (e.g., the levitation height) in the cuvette, we assume in eq 3 that the particle does not accelerate ($\vec{a} = 0$) and is moving with its terminal velocity (eq 9). For a spherical particle, $V = (4\pi/3)R^3$, and the force of the viscous drag \vec{F}_d is given by eq 10, where η (kg m⁻¹ s⁻¹) is the dynamic viscosity of the suspending medium, and \vec{v} is the velocity of the particle (m s⁻¹).

- (21) This is bulk pricing. MnCl₂ and GdCl₃ can be purchased from Sigma Aldrich for \$0.14 and \$2.30 per gram, respectively; it costs about \$0.10 to fill a 4-mL cuvette with a 1 M aqueous solution of MnCl₂ purchased from Sigma Aldrich (the concentration used for typical experiments in this paper).
- (22) Shevkopylas, S. S.; Siegel, A. C.; Westervelt, R. M.; Prentiss, M. G.; Whitesides, G. M. *Lab Chip* **2007**, *7*, 1294–1302.

- (23) Engel-Herbert, R.; Hesjedal, T. *J. Appl. Phys.* **2005**, *97*, 074504.
- (24) Guo, X. F.; Yang, Y.; Zheng, X. *J. Appl. Math. Mech.-Engl. Ed.* **2004**, *25*, 297–306.
- (25) Giancoli, D. C. *Physics: Principles and Applications*; Prentice Hall: Upper Saddle River, NJ, 2004.

$$\vec{F}_{\text{mag}} + \vec{F}_g + \vec{F}_d = 0 \quad (9)$$

$$\vec{F}_d = -6\pi\eta R\vec{v} \quad (10)$$

After substituting eqs 4, 10, and 6 into eq 9, we express its z component by eq 11a; integration of eq 11a yields the time t_0 (s) the particle takes to reach z_f (eq 12). Because the velocity of the particle (eq 11a) approaches zero as the particle moves closer to its equilibrium levitation height h (eq 7), the particle never reaches h in our model (i.e., $t_0 = \infty$ when we evaluate eq 12 for $z_f = h$).

$$\frac{dz}{dt} = \xi z + \zeta \quad (11a)$$

$$\xi = \frac{8R^2 B_0^2}{9\mu_0 d^2 \eta} (\chi_s - \chi_m) \quad (11b)$$

$$\zeta = -\frac{2R^2}{9\eta} \left((\rho_s - \rho_m)g + \frac{2B_0^2}{\mu_0 d} (\chi_s - \chi_m) \right) \quad (11c)$$

$$t_0 = \frac{1}{\xi} \ln \left(\frac{\xi z_f + \zeta}{\xi z_i + \zeta} \right) \quad (12)$$

Minimum Size Required for a Particle To Reach a Stable Equilibrium. In the derivation of eq 8a, we have implicitly assumed that gravitational and magnetic forces dominate and that the effect of thermal motion on macroscopic behavior of the sample object can be neglected. For sufficiently small particles (e.g., molecules) this assumption is clearly incorrect. We can estimate the limit of validity of this assumption, and the size of the objects required in this method to avoid errors, by comparing the energies of the gravitational (U_g) and the magnetic (U_m) interactions with thermal energy (E_T) in our system (eq 13). By solving the inequality in eq 13 and assuming that the shape of the object is spherical, we find the lower limit for the radius of the spherical object for which the assumption holds (eq 14) by estimating the size at which $U_g + U_m \geq 10(k_B T)$. We evaluate this claim experimentally in the Results and Discussion section. In practice, we estimate that $R > \sim 2 \mu\text{m}$ is necessary for a reliable correlation of levitation height with density.

$$U_g + U_m = (\rho_s - \rho_m)Vgz - \frac{(\chi_s - \chi_m)V}{\mu_0} (\vec{B} \cdot \vec{B}) \gg k_B T = E_T \quad (13)$$

$$R \gg \left(\frac{k_B T}{\frac{4\pi}{3} \left((\rho_s - \rho_m)gz - \frac{(\chi_s - \chi_m)}{\mu_0} \left(-\frac{2B_0}{d}z + B_0 \right)^2 \right)} \right)^{1/3} \quad (14)$$

Assumptions of the Model. In deriving the model (eq 8a), we made five assumptions and approximations regarding the magnetic field between the magnets and the properties of the materials: (i) we assumed precise alignment of the magnets on top of one another; (ii) we neglected the x and y components of the magnetic field (as well as their derivatives) and approximated the dependence of the z component of the field on the distance from the bottom magnet with a linear relationship (eq 6); (iii) we ignored the effects of the shape of the container enclosing the paramagnetic medium and of the particle itself on the magnetic field; (iv) we assumed that the bulk magnetic susceptibility of the paramagnetic medium (χ_m) and the bulk diamagnetic susceptibility of the sample (χ_s) are both uniform and homogeneous;³ and (v) we assumed that densities of the paramagnetic medium and of the particle remain constant on the time scale of our measurements (seconds to hours) at 23 °C.

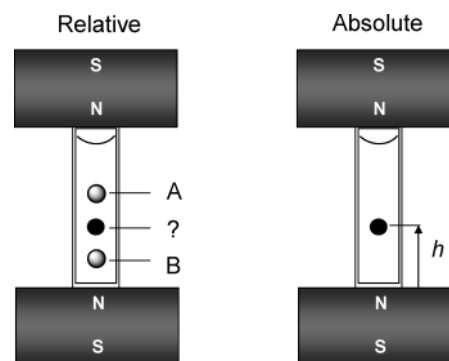


Figure 2. Comparing relative and absolute approaches for measuring densities with magnetic levitation.

Types of Measurements. In general, to measure density using magnetic levitation (Figure 1), we add a particle or a drop of liquid to a vial containing the paramagnetic medium, place the vial between the two magnets, allow sufficient time for the particle to relocate to its equilibrium position (1 s to 100 min, depending on the size of the analyte), measure the levitation height, and compute the density of the sample using eq 8a. A precise alignment of the main axis of the vial containing the suspension of sample particles with the centerline between the magnets is not necessary (Figure 1). Because in the xy plane an effectively *diamagnetic* particle (for which $\chi_s - \chi_m < 0$) will be attracted to the minimum of the magnetic field, the particle will tend to move toward the centerline (the dotted line in Figure 1a,c); that is, the particle will *self-align* with the centerline of the system and will automatically correct for the imperfect placement of the vial (see Figure S3 in the Supporting Information).

Equation 8a applies only when the sample particle levitates between the magnets. Sinking of the particle all the way to the bottom of the vial would indicate that $\rho_s \gg \rho_m$ and/or that $\chi_s > \chi_m$; floating of the particle to the top of the vial would indicate that $\rho_s \ll \rho_m$ and/or that $\chi_s > \chi_m$.²⁶

a. Measurements of Density with Calibrated Standards. The simplest way to measure unknown densities by magnetic levitation is to first levitate objects with *known* densities, measure their levitation heights, determine the values of parameters α and β in eq 8a empirically, and then use these values for computing the unknown densities from the levitation heights of the sample particles (Figure 2). An attractive feature of this approach is that it does not require an accurate knowledge of individual experimental parameters in eq 8a or detailed understanding of the physics of magnetic levitation.

Since the density of most solids and liquids is a function of temperature, the system must be calibrated with appropriate density standards valid for a specific range of temperatures. Many common organic and inorganic substances (polymers, organic droplets, etc.) have well-characterized densities and can be used as density standards. This approach for measuring densities neglects the difference in magnetic susceptibilities between the density standards and the sample analytes (differences in magnetic susceptibilities for most diamagnetic substances are small; see Figure S2 in the Supporting Information for typical values). The accuracy of these measurements, therefore, depends only on the linearity of the field gradient, the precision with which one knows the density of the standards used for generating the calibration curve, and the accuracy of the measurements of the equilibrium levitation heights.

To estimate the error in the measurements of density based on calibration curves, we assume that we know the calibration

(26) The differences between ρ_s and ρ_m depend on exact experimental conditions. Large values of χ_m ($\sim 10^3$) tolerate large differences in $\Delta\rho$ ($\sim 0.02 \text{ g/cm}^3$), whereas small values of χ_m ($\sim 10^5$) tolerate small differences in $\Delta\rho$ ($\sim 0.002 \text{ g/cm}^3$). Particles levitate within the device as long as $\chi_m > \chi_s$.

Table 1. Summary of the Experimental Parameters, and Their Associated Uncertainties, Used in Calculating ρ_s Using Eq 8a

parameter P	description	typical magnitude of P used in this study ^a	δP^b	$\delta\rho_s(P)^c$ (g/cm ³)
Experimental Parameters				
B_0	strength of magnetic field at the surface of the magnet	0.375 T	± 0.003 T	$\pm 0.00001-0.007$ T
d	distance between magnets	45 mm	± 0.5 mm	$\pm 0.000002-0.02$ mm
T	Temperature	23 °C	± 1 °C	± 0.0003 °C
c	concentration of MnCl ₂	0.100–5.000 M	± 0.002 M	± 0.0003 M
Unknown				
χ_s	bulk magnetic susceptibility of the sample	-5×10^{-6} (SI, unitless)	$\pm 10 \times 10^{-6}$	$\pm 0.0001-0.005$
Calculated Parameters				
$\rho_m(c,T)$	density of paramagnetic medium	1.01–2.22 g/cm ³	± 0.0005 g/cm ³	± 0.0005 g/cm ³
$\chi_m(c,T)$	bulk magnetic susceptibility of the medium	$10^{-5}-10^{-3}$ (SI, unitless)	$\pm 1 \times 10^{-6}$	$\pm 0.00001-0.0005$
Constants				
g	acceleration due to gravity	9.80 m/s ²	n/a	n/a
μ_0	permeability of free space	$4\pi \times 10^{-6}$ N·A ⁻²	n/a	n/a
Independent Variable				
h	“levitation height” of the sample above the bottom magnet	0–45 mm	± 0.5 mm	$\pm 0.0002-0.01$ mm
Dependent Variable				
ρ_s	density of sample	1.01–2.28 g/cm ³		$\pm 0.0002-0.02$ g/cm ³ ^d

^a We give a *range* of values because the uncertainty in ρ_s depends on the value of specific experimental parameters used for measurement; the given range is constrained by the typical variation in c (0.1–5 M MnCl₂) and h (0–45 mm). ^b Magnitude of uncertainty in P . ^c Magnitude of uncertainty in ρ_s as a function of each individual P . $\delta\rho_s(P) = |\partial\rho_s/\partial P|\delta P$. ^d Resulting uncertainty in ρ_s as defined by eq 16.

parameters α and β exactly and treat ρ_s as a function of only one variable, h ; we use eq 15 to propagate the uncertainty in ρ_s .²⁷

$$\delta\rho_s = \left| \frac{d\rho_s}{dh} \right| \delta h = |\alpha| \delta h \quad (15)$$

b. Direct Measurements of Density Using Eq 8a. A second way to measure unknown densities is to apply eq 8a directly: that is, to evaluate α and β using parameters of the system, measure the levitation height of the particle of interest, and then compute the density of the sample (Figure 2). This type of measurement can be performed without objects with known densities as standards but requires considerations of the assumptions associated with the physics of the system, as well as an accurate knowledge of the parameters of the system, including ρ_m , h , d , χ_m , χ_s , and B_0 , and their dependence on and sensitivity to a number of environmental influences. With an accurate knowledge of these parameters, however, eq 8a provides easy access to routine density measurements using magnetic levitation without any need for density standards.

Table 1 summarizes the typical range of values of experimental parameters used in this study, the uncertainties associated with each of them, and their effect on $\delta\rho_s$ (assuming that all other parameters are known exactly). The Supporting Information provides a detailed discussion of how these parameters were measured and calculated and of the uncertainties and assumptions associated with each one of them.

To estimate the uncertainty of measurement ($\delta\rho_s$) based on the direct use of eq 8a, we treat ρ_s as a function of the following variables: B_0 (measured in an assembled device using a magnetometer), d and h (both measured using a ruler with millimeter scale markings), c (concentration of the paramagnetic salt in paramagnetic medium, calculated from the mass of salt dissolved in a specified volume of liquid), and T (ambient temperature measured using a thermometer). We compute $\rho_m(c,T)$ and $\chi_m(c,T)$ using the well-known empirical dependencies of densities and magnetic susceptibilities for aqueous salt solutions on concentration and temperature^{3,28,29} (see Supporting Information for details) and use these calculated values of ρ_m and χ_m in eq 8a. We assume that $\chi_s = -5 \times 10^{-6}$ and that differences in magnetic susceptibilities between various diamagnetic substances are negligible (this assumption should hold for most common diamagnetic substances; see Sup-

porting Information for a detailed discussion). We treat each of these variables as a source of an independent random error and use a standard expression given by eq 16 to estimate $\delta\rho_s$ ²⁷ (we express each of the partial derivatives in eq 16 explicitly in the Supporting Information). The Supporting Information also provides an interactive spreadsheet (Microsoft Excel 2003) based on eqs 8a and 16 that allows the user to estimate $\delta\rho_s$ as a function of specific experimental parameters and uncertainties. As an example, we use eqs 8a and 16 to estimate the effect of uncertainty in temperature of ± 10 °C (in case a user does not have access to a thermometer for a more accurate measurement of T) and in the value of B_0 of ± 0.1 T (in case a user does not have access to a magnetometer for measurement of B_0 and has to rely on the value provided by the manufacturer) on the calculated uncertainty in ρ_s for polystyrene spheres levitating in 0.350 M MnCl₂ (see Supporting Information).

$$\delta\rho_s = \sqrt{\left(\frac{\partial\rho_s}{\partial T}\delta T\right)^2 + \left(\frac{\partial\rho_s}{\partial c}\delta c\right)^2 + \left(\frac{\partial\rho_s}{\partial\chi_s}\delta\chi_s\right)^2 + \left(\frac{\partial\rho_s}{\partial h}\delta h\right)^2 + \left(\frac{\partial\rho_s}{\partial d}\delta d\right)^2 + \left(\frac{\partial\rho_s}{\partial B_0}\delta B_0\right)^2} \quad (16)$$

Results and Discussion

Misaligning the Vial with the Centerline between the Magnets. The linear relationship between the density of the sample and its equilibrium levitation height described by eq 8a is valid only along the centerline between the two magnets. The convenient feature of this system is that diamagnetic particles levitating within the device *self-align* (in the xy plane) toward the centerline between the magnets (as long as the walls of the container do not prevent them from doing so).

We examined the magnitude of the effect of deliberately misaligning a levitating object away from the centerline (Figure 3A). We levitated a set of five glass beads of standardized, precisely known densities (± 0.0002 g/cm³) in 1.000 M aqueous MnCl₂ and recorded their levitation height (h_s) as a function of

(27) Taylor, J. R. *An Introduction to Error Analysis*; University Science Books: Sausalito, CA, 1997.

(28) Du Tremolet de Lacheisserie, E.; Gignoux, D.; Schlenker, M., Eds. *Magnetism*; Kluwer Academic Publishers: Norwell, MA, 2002.

(29) Sohnel, O.; Novotny, P. *Densities of Aqueous Solutions of Inorganic Substances*; Elsevier: New York, NY, 1985.

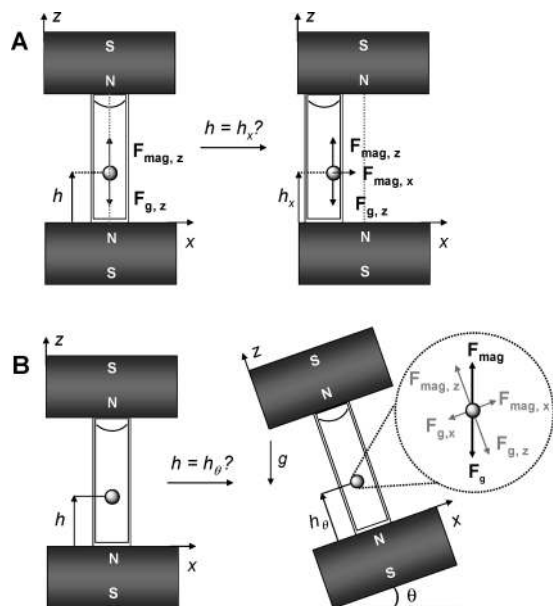


Figure 3. Effect of various experimental parameters on accuracy of measuring densities using magnetic levitation. (A) Effect of displacement of the levitating object away from the centerline between the magnets on its levitation height. (B) Effect of tilting of the experimental setup on the position at which the object levitates.

the horizontal displacement x of the particle away from the vertical centerline between the magnets. We found that in all cases the vertical position of the bead was not affected by displacement away from the centerline and that $h = h_x$. Figure S3 in the Supporting Information illustrates this concept for several different configurations.

Misaligning the Magnetic and Gravitational Forces. The assumption of accurate vertical alignment of magnetic and gravitational forces during measurement is another important feature in eq 8a. Use of the magnetic levitation device in remote environments may make precise vertical alignment of these forces difficult to evaluate. We examined the sensitivity of h to a deliberate misalignment of magnetic and gravitational forces by tilting the device by $\theta = 0\text{--}45^\circ$ (Figure 3B). We levitated a set of five glass beads of precisely known densities in 1.000 M aqueous MnCl_2 and recorded their levitation height (h_θ) as a function of tilt angle θ . We found that $h = h_\theta$ for $\theta \leq 15^\circ$. We also found that the x -component of the gravitational force ($F_{g,x}$) was insufficient to keep the beads that levitated closest to the magnets trapped along the vertical centerline for $\theta > 5^\circ$. For values of $\theta > 25\text{--}45^\circ$, $h < h_\theta$ or $h > h_\theta$ by 2–4 mm for beads levitating above or below (respectively) the vertical center between the two magnets. Figure S4 in the Supporting Information illustrates this result for five glass beads levitating in 1.000 M MnCl_2 at different values of θ . We conclude that small misalignment of the magnetic and gravitational forces due to tilting of the device ($\theta \leq 15^\circ$) will not interfere with the accuracy of the density measurements.

Relationship between the Size of an Object and Its Equilibrium Levitation Height. The balance of magnetic and gravitational forces acting on a particle described by eq 4 determines the position of that particle at equilibrium (eq 7). It also follows from eq 7 that the levitation height of the particle h should not depend on the volume of the particle. Figure 4A shows two polystyrene spheres of different volumes (with radii of 2 and 0.2 mm) levitating at the same height and confirms this prediction.

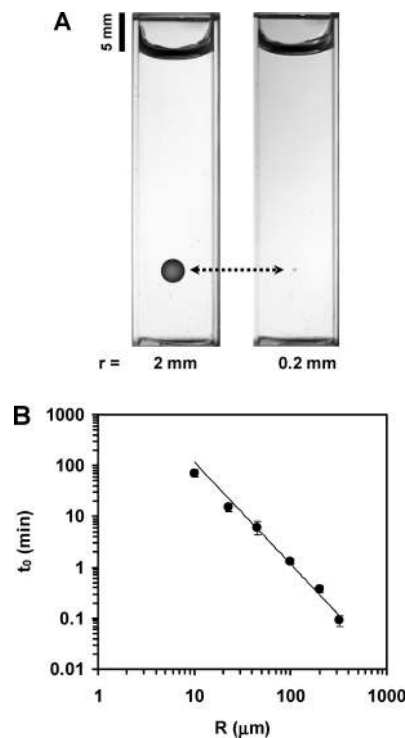


Figure 4. Photographs and plots relating the equilibrium levitation height to the volume of the sample. (A) Photographs of polystyrene spheres ($r = 2$ and 0.2 mm) levitating at 23°C in 150 mM GdCl_3 dissolved in water. The levitation height is independent of the volume of the polystyrene spheres. (B) Graph correlating the radius of polystyrene spheres and the time these spheres take to travel from the bottom of the cuvette ($z_i = 1$ mm) to a levitation height that is close to equilibrium ($z_f = 12$ mm, $|h - z_f| < \delta h$) in aqueous 350 mM MnCl_2 . The vertical error bars denote the standard deviation in time (from seven independent measurements), and the standard deviation in radii provided by the manufacturer is smaller than the size of the data points. The solid line gives the dependence of t_0 on R as predicted by eq 12.

The model predicts that the speed at which particles move toward h depends on size. Figure 4B shows the relationship between the size of the particle and the time it took the particle to approach its equilibrium levitation height h . In this experiment, we placed polystyrene spheres of a particular size into a cuvette filled with an aqueous solution of 350 mM MnCl_2 and 0.05% TWEEN 20 (to prevent the hydrophobic aggregation of the particles) and allowed the spheres to sink to the bottom of the cuvette in the absence of the magnetic field. We then placed the cuvette between the magnets and measured the time it took the particles to travel from the bottom of the cuvette, $z_i = 1$ mm, to a levitation height, $z_f = 12$ mm, that was close to the equilibrium levitation height, h [$|h - z_f| < \delta h$, where δh is the precision of our measurement of heights; according to our model (eq 12) it would take an infinite amount of time for the particles to actually reach the equilibrium levitation height h]. Smaller particles required longer times to reach $z_f = 12$ mm than larger particles (Figure 4B). We could not perform this experiment for particles smaller than $2\ \mu\text{m}$ in radius because these particles (i) remained dispersed evenly throughout the solution and did not sink to the bottom of the cuvette in the absence of the magnetic field and (ii) continued to remain dispersed evenly throughout the solution in the presence of the magnetic field. This dispersion reflects Brownian agitation.

We rationalized the details of this size-dependence in two ways. First, all the forces (\vec{F}_{mag} , \vec{F}_g , and \vec{F}_d) acting on the particle as it moves toward h depend on its size (typical values for the

forces range from 10^{-14} to 10^{-5} N for spherical particles 5–5000 μm in diameter levitating in 350 MnCl_2). The experimental data plotted in Figure 4B correlate well with the prediction of eq 12 for the time required for a particle of a particular size to reach a levitation height close to equilibrium (Figure 4B, solid line). As expected from eq 12, the time required to reach h increases with decreasing size of the particle. Second, eq 12, and our model in general, do not take into account the effect of Brownian motion, which limits the applicability of eq 12 and imposes a lower bound on the size of particles that can be trapped at h . While particles of any size experience numerous collisions with the molecules of the suspending medium, for small ($R < 1\text{--}2$ μm) particles the energy of these interactions becomes comparable to the magnetic and gravitational energy that traps them at h .³⁰ According to eq 14, the radius of the particles must be at least 1 μm (i.e., $R \gg \sim 100$ nm) to be trapped at h within this device at room temperature ($T = 23$ °C). This prediction agrees well with our observation that particles smaller than ~ 2 μm in radius do not localize in a position defined by the balance of the magnetic and gravitation forces, and remain dispersed throughout the container (Figure S5 in the Supporting Information). We observed that particles whose radii were close to this critical value of $R = 1$ μm (i.e., $2\text{--}7$ μm) formed diffuse clouds centered around h and did not localize into the well-defined clusters at h typical for larger particles (Figure S5). We conclude that the apparent levitation height of particles with $R < \sim 2$ μm cannot be used for a reliable estimate of their density.

Effect of Temperature. Several of the parameters in eq 8a, particularly ρ_m and χ_m , depend on temperature; ambient temperature, therefore, will have an effect on the measurements of density using the magnetic levitation technique that must be taken into consideration. For measurements of density made relative to a calibration curve, one will simply need to obtain and use calibrated density standards valid for a specific temperature range. For absolute measurements that rely on the physics of magnetic levitation, the user will need to account for the temperature dependence of experimental parameters in eq 8a.

The equations we use for calculating $\rho_m(c,T)$ and $\chi_m(c,T)$ are valid for the temperature range of 5–100 °C and will yield accurate values for these parameters, as long as the appropriate value of T is included in the calculations. To ensure the accuracy of absolute measurements, the user will also need to precalibrate the magnetic field within the device for the specified temperature range using a magnetometer.

We also analyze the effect of temperature dependence on the accuracy of the measurements in the Supporting Information (eq S7, Table S1). This analysis estimates the error in a density measurement obtained as a result of uncertainty in temperature for two hypothetical uncertainties in temperature, ± 1 and ± 10 °C. We find that the uncertainty in temperature of 1 °C propagates (due to the temperature dependence of ρ_m and χ_m) into uncertainty in ρ_s of 0.0003 g/cm^3 , while uncertainty of 10 °C propagates to 0.003 g/cm^3 (see Supporting Information for details).

Relative Densities: Measurements of Density with Calibrated Standards. Comparison of unknowns with calibrated density standards is the simplest approach for measuring density using magnetic levitation. This approach neglects most of the physics of magnetic levitation and does not require accurate knowledge

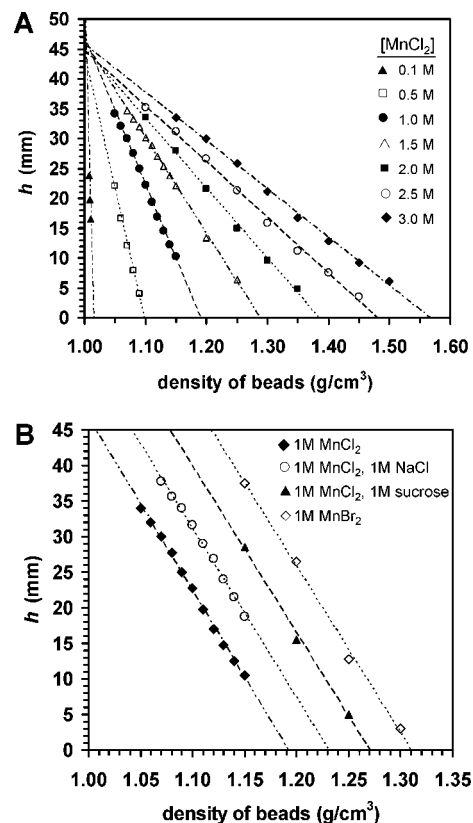


Figure 5. Calibration of the magnetic levitation device with standard density beads. (A) Graph showing the correlation between the density of glass beads and their levitation height at different concentration of aqueous MnCl_2 . The height at which the beads levitate is linearly proportional to the density of the beads (least-squares linear fit from left to right: $h = -3664\rho_s + 3717$, $R^2 = 0.995$; $h = -449\rho_s + 493$, $R^2 = 0.995$; $h = -247\rho_s + 294$, $R^2 = 0.998$; $h = -160\rho_s + 206$, $R^2 = 0.999$; $h = -117\rho_s + 162$, $R^2 = 0.997$; $h = -93.4\rho_s + 138$, $R^2 = 0.997$; $h = -80.8\rho_s + 126$, $R^2 = 0.997$). Each point is the average value from seven independent measurements, and the standard deviation from the average corresponds to the size of the points. (B) Graphs showing the correlation between density of glass beads and their levitation height in aqueous solutions of 1 M MnCl_2 , 1 M MnCl_2 doped with 1 M NaCl, 1 M MnCl_2 doped with 1 M sucrose, and 1 M MnBr_2 .

of most of the experimental parameters. Many commercially available water-insoluble polymers and organic liquids have well-characterized densities and are suitable for use as density standards. Table S0 in the Supporting Information summarizes several types of substances that can be used as density standards in magnetic levitation.

a. Calibrating the System for Measurements of Density. We suspended a set of glass beads of standardized, precisely known densities (± 0.0002 g/cm^3) $\{\rho_{s,i}\}$ in several different concentrations of MnCl_2 dissolved in water (0.100, 0.500, 1.000, 1.500, 2.000, 2.500, and 3.000 M) at 23 °C, measured their levitation positions $\{h_i\}$ to ± 0.5 mm using a ruler with millimeter scale markings, and plotted these two series against one another; the heights at which the beads levitated were linearly proportional to the density of the beads (Figure 5A). We fitted eq 8a to these calibration plots (Figure 5A) to obtain the best-fit values of parameters α and β and then substituted these best-fit α and β into eq 8a to calculate ρ_s of samples of unknown densities on the basis of their h (see the following section). The values of α and β depend on $[\text{MnCl}_2]$; Table S3 tabulates these values, and Figure S6 shows their dependence on $[\text{MnCl}_2]$ (see Supporting Information for details).

(30) Lu, S. S.; Wang, X.; Hirano, H.; Tagawa, T.; Ozoe, H. *J. Appl. Phys.* **2005**, *98*, 114906.

Table 2. Comparison of Density Values Measured by Levitation and Those Obtained from the Vendor or Measured by Helium Pycnometry

sample	density (g/cm ³)			
	obtained from vendor or measured by helium pycnometry	obtained from calibration curves in MnCl ₂	obtained using eq 8a and MnCl ₂	obtained using eq 8a and GdCl ₃
Glass Beads ^a				
1.0100	1.0100 ± 0.0002	1.0099 ± 0.0002	1.010 ± 0.001	1.009 ± 0.001
1.1000	1.1000 ± 0.0002	1.101 ± 0.002	1.101 ± 0.002	1.102 ± 0.002
1.1500	1.1500 ± 0.0002	1.152 ± 0.003	1.152 ± 0.003	1.152 ± 0.003
Spherical Polymers				
polystyrene	1.05 ± 0.01	1.047 ± 0.001	1.047 ± 0.001	1.046 ± 0.001
nylon 6/6	1.14 ± 0.01	1.137 ± 0.002	1.134 ± 0.003	1.136 ± 0.004
poly(methyl methacrylate)	1.18 ± 0.01	1.186 ± 0.004	1.191 ± 0.005	1.185 ± 0.003
Irregularly Shaped Polymers				
polystyrene	1.051 ± 0.001	1.049 ± 0.001	1.050 ± 0.001	1.045 ± 0.003
poly(styrene-co-acrylonitrile)	1.080 ± 0.001	1.076 ± 0.002	1.078 ± 0.003	1.076 ± 0.003
poly(styrene-co-methyl methacrylate)	1.137 ± 0.001	1.133 ± 0.002	1.132 ± 0.003	1.132 ± 0.002
Organic Droplets				
chlorobenzene	1.107	1.115 ± 0.003	1.115 ± 0.002	1.100 ± 0.003
2-nitrotoluene	1.163	1.169 ± 0.003	1.166 ± 0.005	1.157 ± 0.003
dichloromethane	1.325	1.324 ± 0.006	1.329 ± 0.007	1.300 ± 0.007
3-bromotoluene	1.410	1.405 ± 0.006	1.416 ± 0.007	1.404 ± 0.006
chloroform	1.492	1.479 ± 0.007	1.488 ± 0.008	1.471 ± 0.006

^a We had duplicates of various glass beads from the vendor. We used one set of beads to generate the calibration plots in Figure 5. We then used duplicated beads as “unknowns” to test the accuracy of the method.

The magnetic susceptibility of the medium, χ_m , determined the slope of each line in Figure 5A. The slope of each line also revealed the relationship between χ_m and the resolution of the method and its sensitivity to differences in density. While the sensitivity and the resolution are higher at low values of χ_m , only a limited range of densities can be measured and compared within the same paramagnetic solution. Conversely, while the sensitivity and the resolution are lower at higher values of χ_m , a wider range of densities can be measured within the same solution. Because resolution in h increases with decreasing χ_m , we conclude that the most accurate measurements of ρ_s will be obtained at low values of χ_m , such that $\rho_s \approx \rho_m$ and $\chi_m \approx 10^{-5}$.

We determined experimentally that the minimum value of χ_m required for levitation of diamagnetic particles was $\sim 4 \times 10^{-6}$ for objects with $R = 1\text{--}2$ mm; this value corresponded to ~ 10 mM GdCl₃ or ~ 20 mM MnCl₂. Below this value, the diamagnetic particles (depending on their density relative to the density of the medium) either sank to the bottom ($\rho_s > \rho_m$), floated at the surface of the liquid at the top of the container ($\rho_s < \rho_m$), or floated at any position within the container ($\rho_s \approx \rho_m$). Experiments at this minimum value of χ_m were very sensitive to environmental conditions—even a modest change in temperature (for example, caused by touching the container with a finger) was sufficient to change the levitation height of a diamagnetic particle. At higher concentrations of paramagnetic salt (50 mM GdCl₃ and 100 mM MnCl₂), the system was much less sensitive to such perturbations and was, therefore, more suitable for accurate and reliable measurements of density.

Since one of our goals was to develop a *simple* technique for measuring density (e.g., for use in resource-poor settings), we used an ordinary ruler (with 1 mm marks) to measure the levitation height of the diamagnetic objects. The use of the ruler limited the accuracy of our measurements of h to ± 0.5 mm—this value of uncertainty is one of the factors that limited the precision of our measurements of densities using the calibration curves to ± 0.0002 g/cm³ (for media with 50 mM GdCl₃ or 100 mM MnCl₂).

Another factor that limited the accuracy is the uncertainty associated with the densities of the standards that we used for

calibrating the device. We calibrated the device using a set of standards with densities known to ± 0.0002 g/cm³ at 23 °C. These standards—purchased from American Density Materials—are certified according to the methods prescribed by ASTM, using measures and weights traceable to NIST. The accuracy of our measurements, therefore, cannot exceed the accuracy of the available standards.

b. Measuring Densities of Spherical Solids Using Calibrated Standards. We evaluated the accuracy of the method by levitating three glass beads and three spherically shaped polymeric beads and determining their densities using the calibration plots (Figure 5A) generated for aqueous solutions of MnCl₂. We used methods described above to calculate the error associated with each measurement; Table 2 summarizes the results of these calculations (see Table S4 in the Supporting Information for additional details). Densities measured using this method correlated with the values provided by the vendors of the samples and with values obtained using a helium pycnometer within the 95% confidence interval (Table 2).

c. Measuring Densities of Irregularly Shaped Polymers Using Calibrated Standards. We also evaluated the accuracy of the method by levitating three irregularly shaped polymers that were about 4 mm in diameter (Table 2). We assumed that all of the objects in this study were uniform in density and that the approximate vertical midpoint of the levitating object corresponded to h . We tested the accuracy of this assumption by levitating seven different samples from each stock of irregularly shaped polymers and approximated the levitation height each time using a ruler. In all of our measurements, the uncertainty in h did not exceed the uncertainty of ± 0.5 mm imposed by using a ruler, and the density values obtained by levitation correlated with those obtained by helium pycnometry within the 95% confidence interval (Table 2).

We conclude that the uncertainty in h due to irregularity in shape is insignificant for small objects (less than ~ 4 mm in diameter) of uniform density, while for larger particles it may lead to an increased error in ρ_s . For even smaller objects (< 1 mm in diameter), the uncertainty in h due to the uncertainty of locating the center of mass is even smaller.

d. Measuring Densities of Organic Droplets Using Calibrated Standards. We also tested this method by levitating five samples of organic liquids within the device (Table 2). We injected individual droplets ($\sim 5 \mu\text{L}$) of these organic liquids with a syringe into a vial containing an aqueous paramagnetic solution and centered the vial between the two NdFeB magnets. The immiscible organic droplets reached their equilibrium “levitation height” within seconds and levitated stably within the device with no apparent change in h for at least 30 min. We approximated the levitation height of each droplet using a ruler and calculated the density of each liquid using the calibration plots and eq 8a. We found that the values of density obtained by levitation correlated with those provided by the vendor within the 95% confidence interval. The success of this experiment also indicates that commercially available, pure, water-insoluble organic liquids with known densities can be substituted for expensive density standards when calibrating the system.

e. Adjusting the Density of the Paramagnetic Medium. The ability to levitate diamagnetic samples—and therefore, the range of densities that can be measured using this technique—depends on the values of ρ_m and χ_m . Figure 5A shows that the value of χ_m also dictates the sensitivity and resolution of the technique to differences in densities. Both ρ_m and χ_m depend on the concentration of paramagnetic ions in solution. Therefore, it is not possible to change either one of these parameters independently simply by varying the concentration of the paramagnetic ions in solution. The density of the medium ρ_m can, however, be modulated independently by varying the concentration of diamagnetic ions in solution.

Figure 5B illustrates that it is possible to alter ρ_m without significantly changing χ_m by adding diamagnetic cosolutes to the paramagnetic medium. We set the value of χ_m at $\sim 1.8 \times 10^{-4}$ by adjusting the concentration of Mn^{2+} to 1.000 M and varied ρ_m by adding 1.000 M NaCl or 1.000 M sucrose to the MnCl_2 solution or by changing the diamagnetic anion of the paramagnetic salt (e.g., using 1.000 M MnBr_2 instead of MnCl_2). We prepared these solutions by dissolving the desired mixtures of salts within the same volumetric flask to ensure accurate concentrations of all the ions in the final solution. The results in Figure 5B indicate that varying the concentration or the type of diamagnetic ions in solution allows control over ρ_m that is independent of control over χ_m .

We measured densities of objects in the range of 1.0–1.7 g/cm^3 using solutions of MnCl_2 and GdCl_3 in water. In principle, the density of common aqueous solutions of salts can vary in a wider range of 1–3 g/cm^3 .³¹ For instance, doping aqueous 3.0 M MnBr_2 solution with 3.8 M ZnBr_2 enabled levitation of Teflon ($\rho_s = 2.20 \text{ g}/\text{cm}^3$), borosilicate glass ($\rho_s = 2.24 \text{ g}/\text{cm}^3$), and a droplet of iodomethane ($\rho_s = 2.28 \text{ g}/\text{cm}^3$). Therefore, we expect that doping the paramagnetic medium with various types of diamagnetic cosolutes should permit levitation and measurement of densities of samples that range from 1 to $\sim 3 \text{ g}/\text{cm}^3$.

Figure 6 shows an estimate of the range of densities accessible to this technique by using pure aqueous solutions of MnCl_2 , GdCl_3 , and CuSO_4 alone and in combination with other salts. The V-shape of the curves is constrained by the range of densities that can be levitated at a given value of χ_m within a 4.5-cm-tall cuvette positioned between the magnets (4.5 cm apart), and the upper limit is determined by the solubility limit of these salts in water.

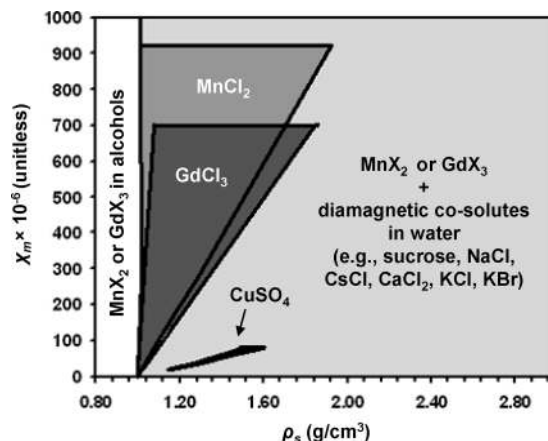


Figure 6. Accessible range of densities ρ_s that can be measured by levitating samples in paramagnetic salt solutions between two NdFeB magnets (5 cm \times 5 cm \times 2.5 cm) positioned 4.5 cm apart. The V-shape of the curves is constrained by the range of densities that can be levitated at a given value of χ_m within a 4.5-cm-tall cuvette positioned between the magnets (4.5 cm apart), and the upper boundary is established by the solubility limit of these salts in water.

Salts of Gd^{3+} and Mn^{2+} are also soluble in alcohols¹⁷ and other polar organic solvents (e.g., *N,N*-dimethylformamide and dimethylsulfoxide) that have densities higher or lower than the density of water. Solutions of GdCl_3 and MnCl_2 in these solvents could expand the range of densities that can be measured with magnetic levitation to 0.8–3 g/cm^3 .

Direct Measurements of Density Using Eq 8a. Equation 8a enables a direct calculation of ρ_m in the absence of calibration curves, provided that all of its parameters are known. We evaluated the accuracy of this method by levitating three glass beads, three spherically shaped polymers, three irregularly shaped polymers, and five different organic droplets in aqueous solutions of MnCl_2 and GdCl_3 . The size of these objects did not exceed ~ 4 mm in diameter; as discussed above, for this size of the objects the error in h due to irregularity in shape did not exceed ± 0.5 mm. Table 2 summarizes the results and compares the accuracy of this approach to that of the approach involving calibration curves (Tables S4–S6 in the Supporting Information provide additional details).

Guidelines to the User. a. Understanding the Accuracy of the Method. The origin of the high accuracy of this method (for both relative and absolute measurements) can be understood in two ways: qualitatively (using the balance of forces required for levitation) and quantitatively (using the rules of error analysis). Both explanations take into account the fact that ρ_s is a function of multiple experimental parameters— h , ρ_m , d , χ_m , χ_s , and B_0 —and that the uncertainty in ρ_s depends on these parameters and on experimental conditions.

The simplest way to understand the origin of the highest sensitivity observed in specific experiments—when the density of the levitated object is close to that of the paramagnetic fluid—is by considering the basic requirements for levitation of an object in a *dilute* solution of a paramagnetic salt (e.g., 0.1 M MnCl_2) under a relatively *weak* magnetic field (~ 0.4 T) supplied by a permanent NdFeB magnet. To achieve levitation under these conditions, the density of the paramagnetic medium must be closely matched to the density of the levitating object (within $\pm 0.005 \text{ g}/\text{cm}^3$ in 0.1 M MnCl_2). If the density of the medium is mismatched beyond $\pm 0.005 \text{ g}/\text{cm}^3$, the object will not levitate and will either sink or float within the device. This requirement of closely matched and accurately known density

(31) Oster, G.; Yamamoto, M. *Chem. Rev.* **1963**, *63*, 257–268.

is the major reason for the high sensitivity of this technique in dilute paramagnetic solutions. The major part of the measurement is effectively the matching of densities; the magnetic component measures only the last significant figures. In a more concentrated paramagnetic solution of 1 M MnCl_2 , the requirement for closely matched density is relaxed to $\pm 0.09 \text{ g/cm}^3$, which leads to increased uncertainty in calculated density (typically $\sim 0.003 \text{ g/cm}^3$ in 1 M MnCl_2). Figure 5 summarizes the range of densities that can be measured for particular concentrations of MnCl_2 .

Equation 16 describes the calculation of error in ρ_s . For every experimentally determined value of ρ_s , the error will depend on the rate of change (i.e., derivative) of ρ_s with respect to each of the experimental parameters and the uncertainty in that parameter. Figure S7 in the Supporting Information uses this equation to depict graphically the dependence of uncertainty ρ_s on various experimental parameters. The contribution of uncertainty in h to uncertainty ρ_s is significant only at high concentrations of MnCl_2 (i.e., above 1 M MnCl_2 , when the magnetic susceptibility of the medium is high and the density of the medium does not have to be closely matched to the density of the levitating object).

b. Maximum Sensitivity. The maximum sensitivity is obtained at low values of magnetic susceptibility ($\chi_m \sim 10^{-5}$) of paramagnetic medium with the density of the paramagnetic solution closely matched to the density of the analyte. These experimental conditions are ideal for achieving optimized resolution of relative differences in density of up to $\pm 0.0002 \text{ g/cm}^3$, but require, in effect, knowing the approximate density to a high precision ($\pm 0.005\text{--}0.01 \text{ g/cm}^3$) before the magnetic measurement.

c. Maximum Accuracy. Making measurements relative to calibrated density standards at low values of magnetic susceptibility ($\chi_m \approx 10^{-5}$) is the best approach for achieving maximum accuracy. Measurements made in relation to known density standards are particularly useful in the absence of an analytical balance, magnetometer, and thermometer. The disadvantage of this approach is that it relies on the availability of standards of precisely known densities calibrated for the temperature range of operation.

d. Maximum Convenience. Absolute measurements that rely on the physics of magnetic levitation are attractive in situations where the magnetic field within the device and the magnetic susceptibility and density of the medium are known precisely. Absolute measurements in the absence of density standards are most convenient for performing routine measurements of density on a precalibrated device using accurately prepared stocks of paramagnetic solutions. One can easily envisage a field-deployable density measurement kit that consists of a precalibrated device along with several marked plastic containers of paramagnetic solutions. The user would simply drop the sample into the vials to see where it levitates and determine the density of the sample from its levitation height.

Conclusions

This paper describes a device and a method for measuring densities of solids and liquids based on magnetic levitation. The device is inexpensive and easy to operate, and it can be substituted for more sophisticated instrumentation in many routine measurements of density. The measurements can be made either in relation to known density standards (e.g., calibrated glass beads, organic

polymers, immiscible organic droplets) or by using a theoretical expression that relates the density of the sample to its levitation height (eq 8a) in a properly precalibrated system. Measurements made relative to known density standards allow the user to neglect most of the assumptions about the physics of the system, as well as the uncertainties associated with individual experimental parameters in eq 8a.

This method has five useful characteristics: (i) it is compatible with most types of solids and water-immiscible organic liquids, (ii) it provides accurate measurements ($\pm 0.0002\text{--}0.02 \text{ g/cm}^3$) within seconds to minutes, (iii) it is simple and inexpensive (requiring only two permanent NdFeB magnets and a tube filled with a paramagnetic medium), (iv) it operates without electricity, and (v) it is applicable to a wide variety of sample sizes ($10^{-9}\text{--}1 \text{ cm}^3$) and does not require a measurement of either the mass or the volume of the analyte. The method also is capable of measuring several samples simultaneously and resolving samples that contain particles of different densities into separate components.¹⁷

This technique has five limitations: (i) the time required per measurement depends on the size of the analyte, (ii) in the configuration described here, the technique does not reliably measure densities of objects smaller than $\sim 2 \mu\text{m}$ in radius, (iii) the accuracy of the measurements is sensitive to temperature, (iv) the method is not compatible with samples that dissolve or swell in the paramagnetic medium (e.g., aqueous or water-soluble samples), and (v) for highest sensitivity, the density must have been previously determined, since high-sensitivity protocols are applicable only over narrow ranges in $\Delta\rho$.

Magnetic levitation is well-suited to analyze and compare relative differences in density of polymers and other samples that may reflect relative differences in chemical composition or three-dimensional structure. This technique is particularly useful when considerations of cost, simplicity, and portability outweigh precision and accuracy that can be achieved with commercial temperature-controlled density meters.

We expect this technique to find a number of applications in materials and polymer science that may include characterizing materials, monitoring quality of a product produced during a manufacturing process, distinguishing amorphous from crystalline forms of polymeric materials, quantifying percent crystallinity of polymers, and characterizing relative differences in chemical composition of polymers associated with changes in density, such as the extent of cross-linking, loading level of specific functionality, and defects due to entrapment of impurities or air during polymerization.

Acknowledgment. This work was supported by the Bill & Melinda Gates Foundation (no. 51308), a predoctoral fellowship from Eli Lilly (K.A.M.), and postdoctoral fellowships from the Damon Runyon Cancer Research Foundation (S.T.P.) and NIH (S.T.P.). K.A.M. thanks Dr. Raquel Perez-Castillejos, Dr. Eric Mack, Dr. Phillip Snyder, and Dr. Emanuel Carrilho for helpful discussions. M.G. acknowledges a NSEC fellowship under NSF award PHY-0646094.

Supporting Information Available: General methods; additional figures (Figures S0–S7), tables (Tables S0–S6), equations (S0–S9), and references; error analysis; and a spreadsheet for calculation of ρ_s and $\delta\rho_s$. This material is available free of charge via the Internet at <http://pubs.acs.org>.

JA900920S